

Protein Stability—Analysis of Heat and Cold Denaturation without and with Unfolding Models

Joachim Seelig* and Anna Seelig



Cite This: *J. Phys. Chem. B* 2023, 127, 3352–3363



Read Online

ACCESS |



Metrics & More

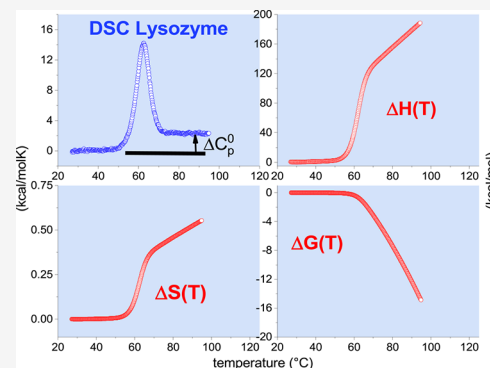


Article Recommendations



Supporting Information

ABSTRACT: Protein stability is important in many areas of life sciences. Thermal protein unfolding is investigated extensively with various spectroscopic techniques. The extraction of thermodynamic properties from these measurements requires the application of models. Differential scanning calorimetry (DSC) is less common, but is unique as it measures directly a thermodynamic property, that is, the heat capacity $C_p(T)$. The analysis of $C_p(T)$ is usually performed with the chemical equilibrium two-state model. This is not necessary and leads to incorrect thermodynamic consequences. Here we demonstrate a straightforward model-independent evaluation of heat capacity experiments in terms of protein unfolding enthalpy $\Delta H(T)$, entropy $\Delta S(T)$, and free energy $\Delta G(T)$. This now allows the comparison of the experimental thermodynamic data with the predictions of different models. We critically examined the standard chemical equilibrium two-state model, which predicts a positive free energy for the native protein, and diverges distinctly from the experimental temperature profiles. We propose two new models which are equally applicable to spectroscopy and calorimetry. The $\Theta_U(T)$ -weighted chemical equilibrium model and the statistical-mechanical two-state model provide excellent fits of the experimental data. They predict sigmoidal temperature profiles for enthalpy and entropy, and a trapezoidal temperature profile for the free energy. This is illustrated with experimental examples for heat and cold denaturation of lysozyme and β -lactoglobulin. We then show that the free energy is not a good criterion to judge protein stability. More useful parameters are discussed, including protein cooperativity. The new parameters are embedded in a well-defined thermodynamic context and are amenable to molecular dynamics calculations.



INTRODUCTION

Many proteins can be denatured by heating or cooling. The detailed knowledge of protein stability is thus an important problem in developing biological therapeutics. A large variety of spectroscopic methods is used to characterize protein unfolding. All these methods reflect structural changes. Their thermodynamic analysis requires the application of models without guaranteeing a correct image of the unfolding thermodynamics. In contrast, the thermodynamic properties of protein unfolding follow directly from the measurement of the heat capacity $C_p(T)$, to which spectroscopic results should then be compared.¹

Here we demonstrate that differential scanning calorimetry (DSC) is the method of choice in analyzing the thermodynamic stability of proteins. The first modern DSC instruments were built independently by Brandts² and by Privalov³ in the 1970s. The heat capacity was found to display a distinct maximum at the midpoint of unfolding. Surprisingly, the scientific interest remained focused on the model-dependent simulation of the heat capacity peak only. Further consequences with respect to entropy and free energy were not considered. We now demonstrate that a simple and model-independent analysis of heat capacity measurements provides all relevant thermodynamic properties of protein stability. Sigmoidal temperature-

profiles are observed for enthalpy and entropy. Due to enthalpy-entropy compensation, the free energy of protein unfolding is small and displays a trapezoidal temperature profile. These model-independent thermodynamic results are used to compare different unfolding models.

Protein unfolding is a cooperative process with many short-lived intermediates. An important co-operative model has been published in 1959, but has largely been ignored.⁴ Instead, a chemical equilibrium two-state model has been proposed for small proteins that has dominated protein unfolding^{2,5–13} for the last 40 years. A two-state model considers only two types of protein conformations in solution, the native protein (N) and the fully unfolded protein (U). Here we compare calorimetric results of heat and cold denaturation of lysozyme and β -lactoglobulin with the predictions of different unfolding models. The standard chemical equilibrium two-state model makes

Received: February 8, 2023

Revised: March 21, 2023

Published: April 11, 2023



incorrect predictions when compared to the experimental results. We therefore introduce two new two-state models. In particular, a statistical-mechanical two-state model yields excellent fits to all observed thermodynamic properties. A modified chemical equilibrium two-state model is also useful for most practical purposes. The new models are equally applicable to calorimetry and spectroscopy. Finally, thermodynamic criteria for protein stability are discussed. Cooperativity appears to be a better indicator of protein stability than changes in free energy.

METHODS

Published protein unfolding data, obtained with differential scanning calorimetry (DSC), are evaluated model-independently in terms of enthalpy, entropy, and free energy by standard thermodynamic methods. The experimental results are then compared to the predictions of two chemical equilibrium two-state models and a statistical model. The focus of the analysis is on the protein unfolding transition proper.

Differential Scanning Calorimetry. “Differential scanning calorimetry (DSC) is a very powerful tool for investigating protein folding and stability because its experimental output reflects the energetics of all conformations that become minimally populated during thermal unfolding.”⁸ In a DSC experiment a sample cell contains the protein solution and a reference cell contains the same buffer. The difference in the amount of heat required to increase the temperature of sample and reference is measured as a function of temperature. Sample and reference are maintained at nearly the same temperature throughout the experiment. DSC allows a precise measurement of the heat capacity $C_p(T)$. In DSC unfolding experiments the protein heat capacity starts almost horizontally reflecting the basic heat capacity of the native protein.¹⁴ Upon unfolding, the heat capacity gives rise to a large heat peak. After unfolding, $C_p(T)$ displays again a smooth increase. Due to the additional binding of water molecules to the backbone and side chains of the unfolded protein, the heat capacity of the unfolded protein is larger than that of the native protein.¹⁵

DSC measurements with modern instruments are straightforward. An excellent review on the use of DSC in protein unfolding has recently been published by Ibarra-Molero et al.⁸ Here, we discuss aspects not included in this review, focusing on the unfolding transition proper. We use published DSC results where the basic heat capacity of the native protein was removed by appropriate baseline correction (for details see ref 8). Hence the native protein has an apparent zero heat capacity. This is without loss of generality as was demonstrated previously.¹⁶

Model-Independent Evaluation of the Heat Capacity $C_p(T)$ with Respect to Enthalpy, Entropy, and Free Energy. According to standard thermodynamics the DSC-measured heat capacity $C_p(T)$ is the derivative of the enthalpy $H(T)$ at constant pressure p .

$$C_p(T) = \left(\frac{\partial H(T)}{\partial T} \right)_p \quad (1)$$

The precise measurement of the temperature profile of the heat capacity $C_p(T)$ provides the thermodynamic functions enthalpy, entropy, and Gibbs free energy. These properties of protein unfolding can be derived model-independently by numerical integration of the standard relations for enthalpy $H(T) = \int C_p(T) dT$, entropy $S(T) = \int \frac{C_p(T)}{T} dT$ and Gibbs free

energy $G(T) = H(T) - TS(T)$. In the DSC experiment the heat capacity is sampled in discrete temperature intervals ΔT and the above integrals can be evaluated as follows:¹⁶

$$\Delta H(T_i)_{\text{DSC}} = \sum_i \left[\frac{C_p(T_i) + C_p(T_{i+1})}{2} \right] [T_{i+1} - T_i] \quad (2)$$

$$\Delta S(T_i)_{\text{DSC}} = \sum_i \left[\frac{C_p(T_{i+1}) + C_p(T_i)}{2T_i} \right] [T_{i+1} - T_i] \quad (3)$$

$$\Delta G(T_i)_{\text{DSC}} = \Delta H(T_i)_{\text{DSC}} - T_i \Delta S(T_i)_{\text{DSC}} \quad (4)$$

These equations define the change of the thermodynamic functions in discrete temperatures steps as will be illustrated in more detail below. Equations 2–4 are of general validity and can also be applied to DSC thermograms, which are not baseline-corrected (see ref 16).

In many published DSC experiments the native and the unfolded protein have the same zero heat capacity.¹⁷ The heat capacity difference ΔC_p^0 between native and unfolded protein is removed by baseline correction. This is unfortunate as “in considering the energetic characteristics of protein unfolding one has to take into account all energy which is accumulated upon heating, [...] that is, all the excess heat effects must be integrated”.¹⁸ The present analysis of experimental data always includes the increased heat capacity ΔC_p^0 .

Models for Protein Unfolding. Protein folding is a conformational reorganization involving the cooperation of many weak local contacts. The concept of “downhill folding” assumes that free energy barriers between protein-like states are intrinsically small^{19,20} in the funnel hypothesis pursued in molecular dynamics calculations. The native protein sits at the bottom of the funnel, which is a minimum of the free energy.

Standard Chemical Equilibrium Two-State Model. The chemical equilibrium two-state model is the long-standing model to analyze calorimetric (DSC) and spectroscopic protein unfolding transitions. It provides the van’t Hoff enthalpy of the $N \rightleftharpoons U$ two-state equilibrium. The model assumes a temperature-dependent equilibrium between a single native protein (N) and a single denatured molecule (U).

$$K_{\text{NU}}(T) = \frac{[U]}{[N]} \quad (5)$$

As the model is well-described (e.g., refs 12, 13) we state the essential thermodynamic equations without further explanation

$$\Delta H_{\text{NU}}(T) = \Delta H_0 + \Delta C_p^0(T - T_m) \quad (6)$$

$$\Delta S_{\text{NU}}(T) = \Delta S_0 + \Delta C_p^0 \ln \frac{T}{T_m} = \frac{\Delta H_0}{T_m} + \Delta C_p^0 \ln \frac{T}{T_m} \quad (7)$$

$$\Delta G_{\text{NU}}(T) = \Delta H_0 \left(1 - \frac{T}{T_m} \right) + \Delta C_p^0 (T - T_m) - T \Delta C_p^0 \ln \left(\frac{T}{T_m} \right) \quad (8)$$

Identical equations in a more complex notation are found in review.⁶

ΔH_0 is the conformational enthalpy (van’t Hoff enthalpy), $\Delta C_p^0 = C_{p, \text{end}} - C_{p, \text{ini}}$ is the heat capacity difference between the

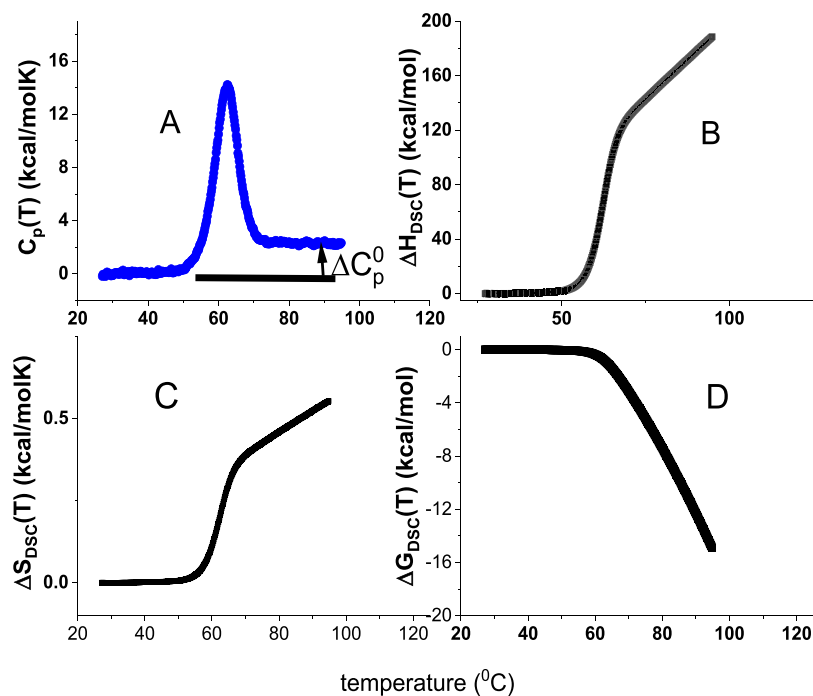


Figure 1. Model-independent evaluation of the molar heat capacity $C_p(T)$ of lysozyme. (A) Primary experimental data. Heat capacity $C_p(T)$ (50 μ M lysozyme, 20% glycine buffer, pH 2.5). DSC data (temperature resolution 0.17 $^{\circ}$ C) taken from ref 1, 26. (B) Enthalpy $\Delta H(T)_{\text{DSC}}$ (eq 2). (C) Entropy $\Delta S(T)_{\text{DSC}}$ (eq 3). (D) Gibbs free energy $\Delta G(T)_{\text{DSC}}$ (eq 4).

native and the unfolded protein. T_m is the midpoint temperature of unfolding.

Equations 6–8 ignore the large heat capacity peak of the unfolding reaction at T_m (see Figure 1A). Differential scanning calorimetry shows that the heat capacity of unfolding is a non-linear function of temperature with a pronounced $C_p(T)$ -maximum at T_m . Consequently, the enthalpy $\Delta H(T) = \int C_p(T)dT$ and the entropy $\Delta S = \int \frac{C_p(T)}{T}dT$ are also non-linear functions of temperature. However, in contrast to the experimental observations, eqs 6 and 7 are linear or nearly linear functions.

Equation 8 defines the two-state equilibrium constant

$$K_{\text{NU}}(T) = e^{\frac{-\Delta G_{\text{NU}}(T)}{RT}} \quad (9)$$

and, in turn, the extent of unfolding

$$\Theta_{\text{U}}(T) = \frac{K_{\text{NU}}(T)}{1 + K_{\text{NU}}(T)} = \frac{e^{\frac{-\Delta G_{\text{NU}}(T)}{RT}}}{1 + e^{\frac{-\Delta G_{\text{NU}}(T)}{RT}}} \quad (10)$$

Equation 10 has a sigmoidal shape and is used to fit spectroscopic unfolding transitions. The model has some puzzling consequences. At the midpoint temperature T_m the model predicts $\Delta G_{\text{NU}}(T_m) = 0$ and $\Theta_{\text{U}}(T_m) = 1/2$. Even though only 50% of the protein is unfolded, eqs 6 and 7 predict 100% enthalpy ΔH_0 and 100% entropy ΔS_0 . Another surprise is the positive free energy of the native protein (see Figure 1 in refs^{12,13}). This is against the idea that the native protein constitutes a minimum of the free energy.

The calculation of the heat capacity requires an empirical extension of eq 6, according to $\Delta H_{\text{NU}}(T)\Theta_{\text{U}}(T)$. The heat capacity is then given by

$$\begin{aligned} C_p(T) &= \frac{\partial(\Delta H_{\text{NU}}(T)\Theta_{\text{U}}(T))}{\partial T} \\ &= \Delta H_{\text{NU}} \left(\frac{\partial \Theta_{\text{U}}}{\partial T} \right)_p + \Theta_{\text{U}} \Delta C_p^0 \end{aligned} \quad (11)$$

Equation 11 is identical to eq 14 in ref 6. It provides a good fit of the heat capacity curve of small proteins. However, eq 11 leads to another thermodynamic inconsistency. It predicts a zero heat capacity for the native protein as $\Theta_{\text{U}} = 0$, which is contradicted by nonzero values for enthalpy, entropy and free energy at the same temperature (eqs 6–8). In contrast, DSC confirms zero values of all thermodynamic properties if the heat capacity is zero (see Figure 1).

$\Theta_{\text{U}}(T)$ -Weighted Chemical Equilibrium Two-State Model. This model is a simple extension of the standard model by multiplying eqs 5–7 with the extent of unfolding $\Theta_{\text{U}}(T)$ (eq 10) resulting in three new functions

$$\Delta H_{\Theta}(T) = \Theta_{\text{U}}(T)\Delta H_{\text{NU}}(T) \quad (12)$$

$$\Delta S_{\Theta}(T) = \Theta_{\text{U}}(T)\Delta S_{\text{NU}}(T) \quad (13)$$

$$\Delta G_{\Theta}(T) = \Theta_{\text{U}}(T)\Delta G_{\text{NU}}(T) \quad (14)$$

The heat capacity is given by eq 11. Equations 11–14 define the $\Theta_{\text{U}}(T)$ -weighted chemical equilibrium two-state model, which has not yet been discussed in the relevant literature.

Partition Function. The heat capacity and other thermodynamic properties of protein unfolding are intimately related to the protein partition function $Z(T)$ according to^{21,22}

$$\text{Helmholtz free energy: } F(T) = -RT \ln Z(T), \quad (15)$$

$$\text{Inner energy: } E(T) = RT^2 \frac{\partial \ln Z(T)}{\partial T}, \quad (16)$$

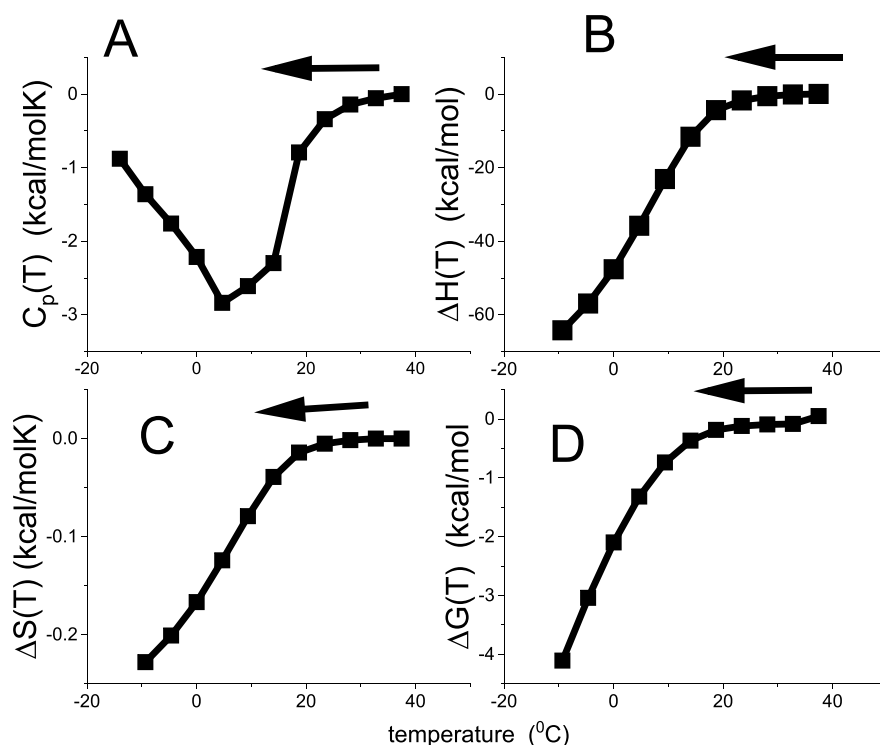


Figure 2. Cold denaturation of β -lactoglobulin. Data in panel A are taken from ref 41, Figure 2, 4 M urea. The arrows indicate the cooling direction. The DSC experiment starts with the native protein at ~ 35 °C and the temperature is reduced linearly to -14 °C. The heat capacity of the native protein is zero due to baseline correction. (A) Heat capacity $C_p(T)$. (B) Enthalpy $\Delta H_{\text{DSC}}(T)$. (C) Entropy $\Delta S_{\text{DSC}}(T)$. (D) Gibbs free energy $\Delta G_{\text{DSC}}(T)$.

$$\text{Entropy: } S_v(T) = \frac{E(T) - F(T)}{T}, \quad (17)$$

$$\text{Heat capacity: } C_v(T) = \left(\frac{\partial E(T)}{\partial T} \right)_v = \frac{\langle E(T)^2 \rangle - \langle E(T) \rangle^2}{RT^2} \quad (18)$$

Equations 15–18 refer to reactions at constant volume. Volume changes in protein unfolding are rather small ($\leq 5\%$).²³ Hence the following identities hold: $\Delta E \cong \Delta H$, $\Delta S_v \cong \Delta S_p$, $\Delta F \cong \Delta G$.

Statistical-Mechanical Two-State Model. Macroscopic Parameters. We present a simple statistical-mechanical two-state model as an alternative to the chemical equilibrium two-state model. Based on the statistics of the linear Ising model²⁴ as described in ref 25 the following continuous canonical partition function can be defined²⁶

$$Z(T) = 1 + e^{-\left(\frac{\Delta E_0 + C_v(T - T_0)}{R} \right) \left(\frac{1}{T} - \frac{1}{T_0} \right)} \quad (19)$$

ΔE_0 is the difference in inner energy between the native and the unfolded protein. ΔE_0 is virtually identical to the conformational enthalpy ΔH_0 as will be shown experimentally below. The inner energy ΔE_0 is temperature-dependent with the heat capacity C_v , which accounts for the increase ΔC_p^0 between the native and the denatured protein. The partition function $Z(T)$ predicts all thermodynamic properties, in combination with eqs 15–18. The extent of unfolding is not needed in the calculation of thermodynamic properties and is given here for completeness only

$$\Theta_U(T) = \frac{Q(T)}{1 + Q(T)} \quad (20)$$

$$\text{with } Q(T) = e^{-\left(\frac{E_0 + C_v(T - T_m)}{R} \right) \left(\frac{1}{T} - \frac{1}{T_m} \right)}.$$

The statistical-mechanical two-state model provides an analytical expression for the temperature of cold denaturation. The midpoint of unfolding is

$$T_{\text{cold}} = T_m - \frac{\Delta E_0}{C_v} \quad (21)$$

ΔE_0 and C_v have opposite effects on T_{cold} : ΔE_0 stabilizes the protein and lowers T_{cold} , C_v represents energy fluctuations (eq 19), destabilizing the structure and increasing T_{cold} .

Multistate Cooperative Unfolding Model. Molecular Parameters. The partition function determines the thermodynamic properties of the system (eqs 23–26).^{21,22} We use the partition function of the multistate cooperative Zimm–Bragg theory.^{4,27,28} The Zimm–Bragg theory has been applied successfully to the unfolding of helical and globular proteins of different structure and size.^{1,16,26,29–34} Here we use¹⁶

$$Z(T) = (1 \ 0) \begin{pmatrix} 1 & \sigma q(T) \\ 1 & q(T) \end{pmatrix}^N \begin{pmatrix} 1 \\ 1 \end{pmatrix} \quad (22)$$

$$q(T) = e^{-\left(\frac{h(T)}{R} \right) \left(\frac{1}{T} - \frac{1}{T_m} \right)} \quad (23)$$

$$h(T) = h_0 + c_v(T - T_m) \quad (24)$$

h_0 is the energy change of unfolding a single amino acid. h_0 is temperature-dependent with heat capacity c_v . N is the number of amino acids participating in the transition. The cooperativity parameter σ determines the sharpness of the transition. The smaller σ , the sharper is the transition. σ is typically 10^{-3} – 10^{-6} . Equation 22 can be applied to proteins of any size, even antibodies with unfolding enthalpies of ~ 1000 kcal/mol.¹⁶ In

Table 1. (A–C) DSC Unfolding of Lysozyme and β -Lactoglobulin

parameters	units	DSC	$\Theta_U(T)$ -weighted model	statistical-mechanical model
(A) Thermodynamic Parameter for Lysozyme Heat Unfolding				
T_{ini}^a	°C (K)	45 (318)	45	45
T_m^a	°C (K)	62 (335)	62	62
T_{end}^a	°C (K)	73 (346)	73	73
$\Delta C_p^0, \Delta C_v^b$	kcal/molK	2.27	2.27	1.05
$\Delta H_{DSC}, \Delta H_{\Theta_{total}}, \Delta E_{total}^c$	kcal/mol	137	130.7	132.3
$\Delta H_0, \Delta E_0^d$	kcal/mol		107	110
$\Delta H_{\Delta C_p^e}$	kcal/mol	21.2	23.7	22.3
$\Delta S_{DSC}, \Delta S_p, \Delta S_v^f$	kcal/molK	0.409	0.389	0.394
$\Delta G_{DSC}, \Delta G_0, \Delta F_0^g$	kcal/mol	-4.27	-3.78	-3.87
$\Delta H_{total}/\Delta S_{total}^h$	°C (K)	62 (335)	63 (336)	63 (336)
ΔT^i	°C	n.d.	88	105
(B) Thermodynamic Parameter for β -Lactoglobulin Cold Unfolding				
T_{ini}^a	°C (K)	37 (310)	37	37
T_m^a	°C (K)	6 (279)	7	6
T_{end}^a	°C (K)	-14 (259)	-15	-15
$\Delta C_p^0, \Delta C_v^b$	kcal/molK	0.86	1.1	0.45
$\Delta H_{DSC}, \Delta H_{\Theta_{total}}, \Delta E_{total}^c$	kcal/mol	-69.5	-65	-59.2
$\Delta H_0, \Delta E_0^d$	kcal/mol		-42	-42
$\Delta H_{\Delta C_p^e}$	kcal/mol	-18.9	-23.1	-17.2
$\Delta S_{DSC}, \Delta S_p, \Delta S_v^f$	kcal/molK	-0.248	-0.235	-0.215
$\Delta G_{DSC}, \Delta G_0, \Delta F_0^g$	kcal/mol	-4.1	-4.07	-3.65
$\Delta H_{total}/\Delta S_{total}^h$	°C (K)	8 (280)	3 (276)	3 (276)
(C) Thermodynamic Parameter for β -Lactoglobulin Heat and Cold Unfolding				
T_{ini}^a	°C (°K)	28 (301)	28	28 (301)
T_m^a	°C (°K)	58 (331)	53 (326)	55 (328)
T_{end}^a	°C (°K)	71 (344)	71	71 (344)
$\Delta C_p^0, \Delta C_v^b$	kcal/molK	3.1	2.4	1.25
$\Delta H_{DSC}, \Delta H_{\Theta_{total}}, \Delta E_{total}^c$	kcal/mol	109	99.1	101
nd, $\Delta H_0, \Delta E_0^d$	kcal/mol		56	60
$\Delta H_{\Delta C_p^e}$	kcal/mol	44.3	43	41
$\Delta S_{DSC}, \Delta S_p, \Delta S_v^f$	kcal/molK	0.329	0.286	0.304
$\Delta G_{DSC}, \Delta G_0, \Delta F_0^g$	kcal/mol	-4.12	-4.33	-3.89
$\Delta H_{total}/\Delta S_{total}^h$	K	58 (331)	74 (347)	59 (332)
ΔT^i	°C		47	48
T_{ini}^a	°C (K)	28 (301)	28 (301)	28 (301)
T_{mold}^a	°C (K)	4 (277)	4 (277)	4 (277)
$T_{endcold}^a$	°C (K)	-7 (266)	-7 (266)	-7 (266)
$\Delta C_p^0, \Delta C_v^b$	kcal/molK	2.79	2.4	1.25
$\Delta H_{DSC}, \Delta H_{\Theta_{total}}, \Delta E_{total}^c$	kcal/mol	81.1	87.7	80
$\Delta H_0, \Delta E_0^d$	kcal/mol	56	56	60
$\Delta S_{DSC}, \Delta S_p, \Delta S_v^f$	kcal/molK	0.293	0.331	0.288
$\Delta G_{DSC}, \Delta G_0, \Delta F_0^g$	kcal/mol	-3.06	-4.32	-3.29
$\Delta H_{total}/\Delta S_{total}^h$	°C (K)	4 (277)	-8 (265)	5 (278)

^a T_{ini} , T_m , T_{end} : temperatures of beginning, midpoint, and end of protein unfolding. ^b ΔC_p^0 : total heat capacity change upon unfolding. ΔC_v : heat capacity change of the inner energy E_0 . ^c ΔH_{DSC} : total enthalpy change measured with DSC between T_{ini} and T_{end} . $\Delta H_{\Theta_{total}}$, ΔE_{total} : total heat of unfolding calculated with either the chemical equilibrium model or the statistical-mechanical model. ^d ΔH_0 : conformational enthalpy change. ΔE_0 : conformational inner energy change. ^eContribution of the heat capacity ΔC_p^0 to the total unfolding enthalpy/energy. ^f ΔS_{DSC} : total entropy change measured with DSC between T_{ini} and T_{end} . ΔS_p , ΔS_v : total entropy of unfolding calculated with either the chemical equilibrium model or the statistical-mechanical model. ^g ΔG_{DSC} : total free energy change measured with DSC between T_{ini} and T_{end} . ΔG_0 , ΔF_0 : total free energy of unfolding calculated with either the chemical equilibrium model or the statistical-mechanical model. ^hPrediction of the midpoint of unfolding as the ratio of measured or calculated total enthalpy and total entropy. ⁱPredicted temperature difference between heat to cold denaturation calculated with $\Delta T \approx 2T_0(1 - e^{-\Delta H_0/T_0\Delta C_p^0})$ ($\Theta_U(T)$ -weighted chemical model) and $\Delta T = \Delta E/C_v$ (statistical-mechanical model).

contrast, two-state models are best suited for small proteins with enthalpies of 50–200 kcal/mol.

RESULTS

Lysozyme Heat Unfolding: Thermodynamic Parameters Obtained Model-Independently by DSC. Lysozyme

(14.3 kDa) is a globular 129-residue protein with ~25% α -helix, ~40% β -structure and ~35% random coil in solution at room temperature.¹ Upon unfolding, the α -helix is almost completely lost and the random coil content increases to ~60%. The DSC thermogram of lysozyme unfolding is shown in Figure 1. The baseline-corrected heat capacity $\Delta C_p(T)$ of the native protein is

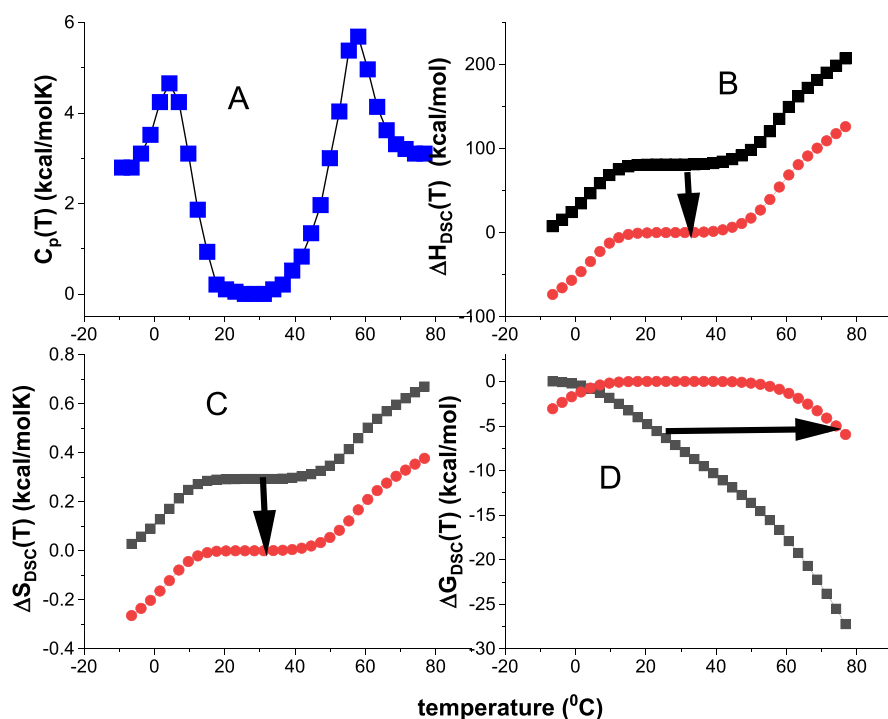


Figure 3. Heat-induced folding (at 4 °C) and unfolding (at 57 °C) of β -lactoglobulin in 2.0 M urea. Model-independent evaluation of the heat capacity $C_p(T)$. (A) DSC data taken from ref 41. (B) Enthalpy $\Delta H_{\text{DSC}}(T)$. Black data points: integration of $C_p(T)$ according to eq 2. Red data points: black data points shifted downwards by 78.3 kcal/mol, the enthalpy of cold denaturation. (C) Entropy $\Delta S(T)_{\text{DSC}}$. Black: integration of $C_p(T)$ with eq 3. Red: primary data points shifted downwards by 0.283 kcal/molK, the unfolding entropy of cold denaturation. (D) Gibbs free energy $\Delta G_{\text{DSC}}(T)$. Black: application of eq 4 to black data points in panels B and C. Red: combination of red data points in panels B and C, according to eq 4.

zero (for detail see ref 16), then goes through a maximum at the midpoint temperature $T_m = 62$ °C and levels off again. The heat capacity increases upon unfolding by $\Delta C_p^0 = 2.27$ kcal/molK. (Literature: 1.54–2.27 kcal/molK^{1,7,15,35–38}). The enthalpy $\Delta H(T)_{\text{DSC}}$ and entropy $\Delta S(T)_{\text{DSC}}$ are evaluated model-independently with eqs 2 and 3 and have sigmoidal shapes (Figure 1B,C). The free energy $\Delta G(T)_{\text{DSC}}$ (eq 4) of the native protein is zero, is slightly negative in the initial phase of unfolding, and decreases rapidly beyond the midpoint temperature $T_m = 62$ °C (Figure 1D).

The total unfolding enthalpy is $\Delta H_{\text{DSC}} = 138$ kcal/mol. It is composed of the conformational enthalpy proper, ΔH_0 and a contribution $\Delta H_{\Delta C_p^0}$ caused by the heat capacity term ΔC_p^0 .

$$\Delta H_{\text{DSC}} = \Delta H_0 + \Delta H_{\Delta C_p^0} \quad (25)$$

The two enthalpies can be separated by applying the models described above. In the model-independent analysis, the contribution $\Delta H_{\Delta C_p^0}$ can be approximated as follows (eq 26).

Equation 26 calculates the area of the triangle defined by the baseline $c_{\text{end}} - c_{\text{ini}}$ and the height ΔC_p^0 . The hypotenuse is a sigmoidal line which explains the factor 3 instead of 2 in the denominator.

$$\Delta H_{\Delta C_p^0} \approx (\Delta C_p^0/3)(T_{\text{end}} - T_{\text{ini}}) \quad (26)$$

The $\Delta H_{\Delta C_p^0}$ values are confirmed by a comparison with the predictions of the $\Theta_U(T)$ -weighted chemical equilibrium model or the statistical-mechanical models. For lysozyme with $\Delta C_p^0 = 2.269$ kcal/mol K, $T_{\text{ini}} = 318$ K, and $T_{\text{end}} = 346$ K this results in $\Delta H_{\Delta C_p^0} = 21.2$ kcal/mol (simulations yield 20–24 kcal/mol). The experimental data for lysozyme are summarized in Table 1A.

Of note, "unfolded" proteins are not completely unfolded, but contain residual structure.^{39,40} Complete unfolding is difficult to achieve as many different physical and chemical factors contribute to protein stability.⁴⁰ In the present evaluation the extent of unfolding is always $\Theta_U > 0.9$ as judged by applying the unfolding models.

β -Lactoglobulin Cold Denaturation—Thermodynamic Parameters Obtained Model-Independently by DSC.

DSC data for cold denaturation are scarce. One of the best examples is the unfolding of β -lactoglobulin in urea solution.⁴¹ Bovine β -Lactoglobulin is an 18.4 kDa protein comprising 162 amino acids that fold up into an 8-stranded, antiparallel β -barrel with a 3-turn α -helix on the outer surface. A DSC cold-denaturation experiment of β -lactoglobulin is shown in Figure 2 (data taken from ref 41). The experiment starts with the native protein at ~ 35 °C and the temperature is lowered gradually to -14 °C. The heat capacity of the native protein is zero and all thermodynamic functions are necessarily also zero at ambient temperature.

Cold denaturation is an exothermic reaction. At the end of the DSC experiment at -14 °C the released heat as evaluated with eq 1 is $\Delta H_{\text{DSC}} = -69.5$ kcal/mol (-291 kJ/mol, in agreement with Table 2 in ref 41). The corresponding entropy change is $\Delta S_{\text{DSC}} = -0.248$ kcal/mol. The ratio $\Delta H_{\text{DSC}}/\Delta S_{\text{DSC}} = 280$ K = 7 °C is close to the experimental $C_p(T)$ minimum at 277 K.

β -Lactoglobulin. Heat-Induced Folding and Unfolding. Thermodynamic Parameters Obtained Model-Independently by DSC. The DSC experiment shown in Figure 3 is unusual as it involves a disorder \rightarrow order transition at low temperature and the reverse order \rightarrow disorder transition at high temperature.

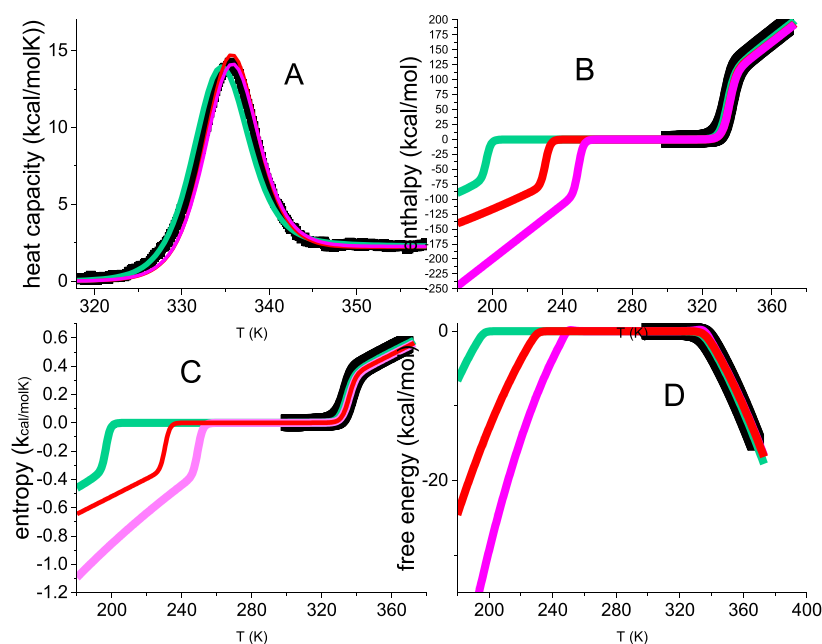


Figure 4. Analysis of lysozyme unfolding with three different models. (■) Experimental DSC results. Same data as in Figure 1. Magenta lines: $\Theta_U(T)$ -weighted chemical equilibrium two-state model. $\Delta H_0 = 107$ kcal/mol, $\Delta C_p^0 = 2.27$ kcal/molK. Red lines: Statistical-mechanical two-state model. $\Delta E_0 = 110$ kcal/mol, $C_v = 1.05$ kcal/molK. Green lines: multistate cooperative model. $h_0 = 0.90$ kcal/mol, $c_v = 7$ cal/molK, $\sigma = 5 \times 10^{-7}$, $N = 129$. (A) Heat capacity. (B) Inner energy $\Delta E(T)$ (green, red), enthalpy $\Delta H(T)$ (magenta). (C) Entropy $\Delta S_v(T)$, $\Delta S_p(T)$. (D) Free energy $\Delta F(T)$, $\Delta G(T)$.

Table 2. Thermodynamic Parameters of the Multistate Cooperative Model¹⁶

parameters	lysozyme	lactoglobulin Figure 6	lactoglobulin/1st peak Figure 7	lactoglobulin/2nd peak Figure 7
h_0 (kcal/mol) ^a	0.91	-0.36	0.58	0.58
c_v (cal/molK) ^b	7	4	17.5	17.5
σ^c	5×10^{-7}	8×10^{-5}	7×10^{-5}	7×10^{-5}
N^d	129	160	80	80
ΔE (kcal/mol) ^e	136.2	-75.5	-76.57	112
ΔS (kcal/molK) ^f	0.406	-0.272	-0.277	0.336
ΔF (kcal/mol) ^g	-4.38	-5.2	-2.76	-4.68
ΔS_{DSC} (kcal/molK) ^h	0.417	-0.248	-0.282	0.313
T_m °C (K) ⁱ	72(335)	5(278)	4(277)	58(331)
$\Delta E/\Delta S$ °C (K) ^j	72 (335) °C	4 (277)	3(276)	60 (333)

^aUnfolding enthalpy per amino acid residue. ^bMolar heat capacity per amino acid residue. ^cCooperativity parameter. ^dNumber of amino acid residues participating in the unfolding transition. ^ePredicted change in the inner energy. ^fPredicted change in the unfolding entropy. ^gPredicted change in the free energy. ^hEntropy change, determined model-independently from DSC data. ⁱMidpoint temperature as determined by DSC. ^jPredicted midpoint temperature from the changes of inner energy and entropy.

Figure 3A reports the DSC experiment. The heat capacity $C_p(T)$ is used to calculate the thermodynamic properties in Figure 3B–D. At the beginning of the DSC experiment at -9 °C, the protein is cold-denatured and disordered. Upon heating, the protein goes through a disorder \rightarrow order transition with a heat uptake of $\Delta H_{DSC} = 78.3$ kcal/mol. At 25 °C the protein is in an ordered, native-like structure. Further heating induces new disorder with an enthalpy uptake of $\Delta H_{DSC} = 104.1$ kcal/mol. $C_p(T)$ shows maxima at 4 and 57 °C. The entropies increase by $\Delta S_{DSC} = 0.3283$ kcal/molK and $\Delta S_{DSC} = 0.313$ kcal/molK, respectively. The ratio $\Delta H_{DSC}/\Delta S_{DSC}$ is 277 K = 4 °C for the disorder \rightarrow order transition and 333 K = 60 °C for heat denaturation, in agreement with the heat capacity maxima.

The blue data points in Figure 3A are integrated with eqs 2–4 result in the black data points in panels 3B–3D. The comparison with cold denaturation in Figure 2 suggests a shift of the enthalpy by -78.3 kcal/mol, the enthalpy of cold denaturation. This scale shift (Figure 3B, red data points) leads to a zero

enthalpy for the native protein and makes Figure 3 consistent with Figure 2. Likewise, the entropy in Figure 3C is shifted by -0.283 kcal/molK. The entropy of the native protein is now also zero. With these scale shifts the recalculated free energy is given by the red data points in Figure 3D. The free energy shows a trapezoidal temperature profile.

Figure 3A is almost a quantitative mirror image of cold-denaturation in Figure 2A. Not surprisingly, the red data points in Figure 3 related to cold denaturation are consistent with the direct measurements in Figure 2.

The experimental thermodynamic data for β -lactoglobulin are summarized in Table 1B.

Analysis of DSC Thermograms with Three Different Models. Lysozyme Heat Unfolding. Figure 4 compares the experimental data of Figure 1 with the $\Theta_U(T)$ -weighted chemical equilibrium two-state model (magenta lines), the statistical-mechanical two-state model (red lines), and the multistate cooperative model (green lines). The simulations cover a large

temperature range, predicting both heat and cold denaturation. However, no experimental data are available for lysozyme cold denaturation. Figure 4A shows virtually identical simulations of the heat capacity by the three models. The conformational parameters of the two-state models are almost identical ($\Delta H_0 = 107$ kcal/mol, $\Delta E_0 = 110$ kcal/mol). The simulation parameters are listed in Table 1B,C for the two-state models and in Table 2 for the multistate cooperative model.

The three models provide good fits of all experimental thermodynamic properties (Figure 4B–D), predicting sigmoidal temperature profiles for enthalpy and entropy and a trapezoidal shape for the free energy. The models show differences with respect to cold denaturation. The statistical-mechanical models predict cold denaturation 20–50 °C lower than the $\Theta_U(T)$ -weighted chemical equilibrium two-state model (cf. Figure 4B,C).

A further difference between the three models is shown in Figure 5, displaying the free energy at enhanced resolution. The

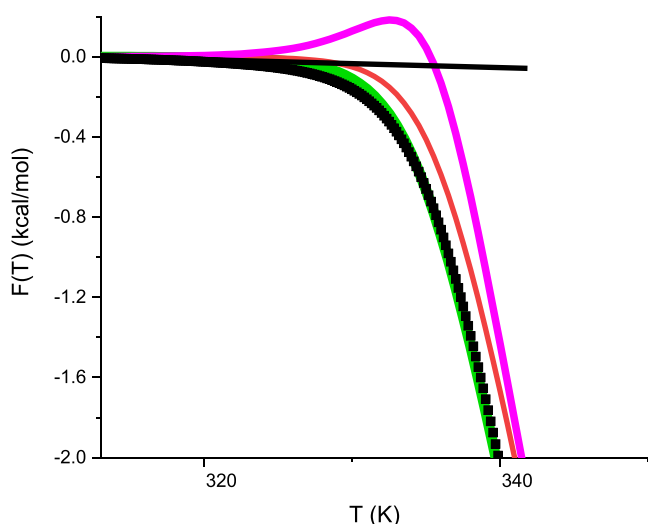


Figure 5. High-resolution temperature profile of the free energy. Black data points: same experimental results for lysozyme as in Figures 1 and 3. Magenta line: $\Theta_U(T)$ -weighted chemical equilibrium model (eq 14, $\Delta H_0 = 107$ kcal/mol, $\Delta C_p^0 = 2.27$ kcal/molK). Red line: statistical mechanical two-state model ($\Delta E_0 = 110$ kcal/mol, $C_v = 1.05$ kcal/molK; eq 16). Green line: multistate cooperative model. ($h_0 = 0.9$ kcal/mol, $c_v = 7$ cal/molK, $\sigma = 5 \times 10^{-7}$, $N = 129$).

DSC experiment reports a zero free energy for the native lysozyme, which becomes immediately negative upon unfolding. Of note, the experimental free energy is always negative, never positive. Both statistical-mechanical models reproduce this result correctly. In contrast, the $\Theta_U(T)$ -weighted chemical equilibrium model displays a small positive peak in the vicinity of T_m . Consequently, the free energies at the midpoint of unfolding are also different. The experimental free energy at $T_m = 62$ °C is $\Delta H(T_m)_{DSC} = -0.76$ kcal/mol. The multistate cooperative model predicts correctly $\Delta F(T_m) = -0.73$ kcal/mol and the statistical-mechanical two-state model $\Delta F(T_m) = -RT_m \ln 2 = -0.46$ kcal/mol. In contrast, the Θ_U -weighted chemical equilibrium two-state model yields exactly $\Delta G_0(T_m) = 0$ kcal/mol. At T_m all three models predict the extent of unfolding as $\Theta_U(T_m) = 1/2$. The protein is partially denatured at T_m and its free energy is necessarily negative.

The parabolic profile of the Gibbs free energy, which is predicted by the standard chemical equilibrium two-state model

(eq 9), deviates even more from the DSC result and is hence not included in Figures 4D–6D.

β -Lactoglobulin. Cold Denaturation Analyzed with Different Models. Cold denaturation is analyzed with three different models. All models provide good fits of the thermodynamic properties. However, the $\Theta_U(T)$ -weighted chemical equilibrium two-state model predicts some positive free energy, which is not supported by the DSC experiment. The multistate cooperative model provides the best simulation.

β -Lactoglobulin. Heat-Induced Folding and Unfolding Analyzed with Different Models. The simultaneous analysis of two heat-induced transitions is shown in Figure 7A for the $\Theta_U(T)$ -weighted chemical equilibrium model (eq 11) and in Figure 7B for the statistical-mechanical models. All three models describe the temperature-profile of the heat capacity $C_p(T)$ equally well.

A criterion for protein stability is the temperature difference between heat and cold denaturation. DSC yields a temperature difference of $\Delta T = 53$ °C between the heat capacity maxima. The prediction of the $\Theta_U(T)$ -weighted chemical equilibrium model is $\Delta T \approx 2T_0(1 - e^{-\Delta H_0/T_0\Delta C_p^0}) = 45$ °C, that of the statistical-mechanical two-state model $\Delta T = \Delta E_0/C_v = 46$ °C, and that of the multistate cooperative model $\Delta T \approx h_0/c_v = 48$ °C.

The simulations of the three models overlap almost completely for heat capacity $C_p(T)$ and enthalpy $\Delta H(T)_{DSC}$ (Figure 7C). In contrast, the free energy prediction of the $\Theta_U(T)$ -weighted chemical equilibrium model deviates from the experimental result in the vicinity of the phase transitions (Figure 7D). The DSC-derived free energy is zero or negative, never positive. The small positive peaks of the $\Theta_U(T)$ -weighted chemical equilibrium two-state model disagree with this experimental result.

The total enthalpy of heat unfolding at 57 °C is $\Delta H_{DSC} = 104$ kcal/mol, but the conformational enthalpy is only $\Delta H_0 = 56$ kcal/mol. The large difference is presumably caused by the binding of urea molecules and is $\Delta H_{\Delta C_p^0} \sim 50$ kcal/mol.

The thermodynamic data and the fit parameters for β -lactoglobulin are summarized in Table 1B,C for the two-state models and in Table 2 for the multistate cooperative model.

DISCUSSION

Model-Independent Analysis of DSC Experiments. The DSC experiment shows peaks of the heat capacity $C_p(T)$ at the temperatures of heat and cold unfolding. No folding model is needed to deduce the thermodynamic properties $\Delta H_{DSC}(T)$, $\Delta S_{DSC}(T)$, and $\Delta G_{DSC}(T)$. The experimental results show sigmoidal curves for enthalpy and entropy and a trapezoidal temperature profile for the free energy. Different unfolding models can then be compared with the experimental data. Of note, the simulation must include not only the heat capacity, but also all three thermodynamic functions. This is ignored in the relevant literature.

Spectroscopy and the Chemical Equilibrium Two-State Model. The chemical equilibrium two-state model is the almost exclusive model to fit spectroscopic unfolding transitions. Recent examples are found for nuclear magnetic resonance (NMR),^{42,43} CD,^{1,44} fluorescence,⁴⁵ Raman spectroscopy,⁴⁶ and elastic neutron scattering.^{47,48} Spectroscopic methods report structural changes, which only indirectly reflect thermodynamic changes. Indeed, a detailed comparison of CD spectroscopy and DSC for 10 different proteins revealed

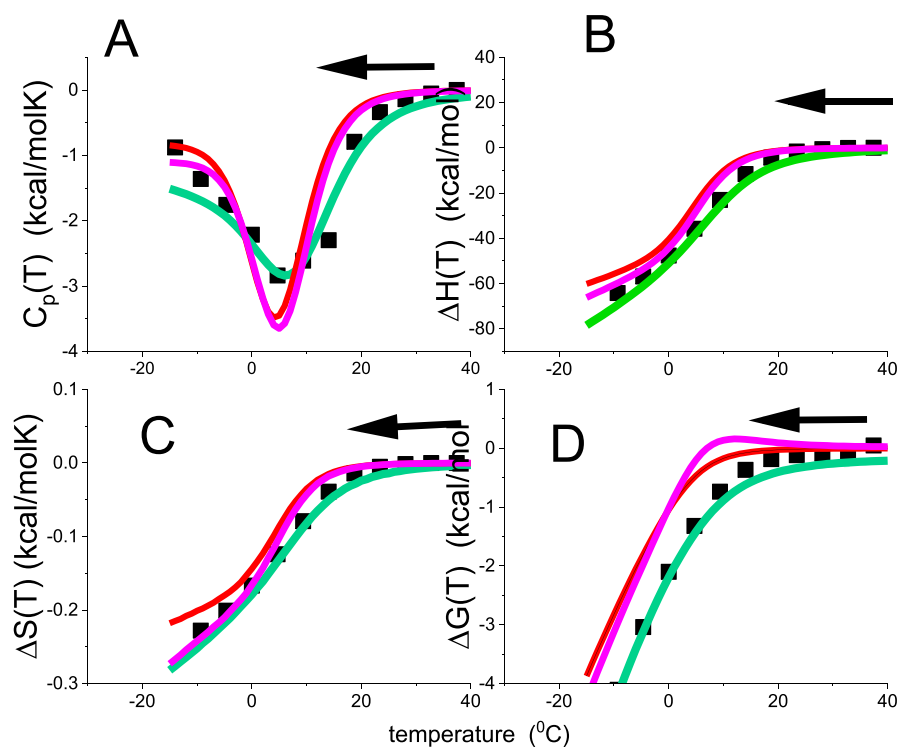


Figure 6. Cold denaturation of β -lactoglobulin. Same experimental data as in Figure 2. Arrows indicate the direction of cooling. The DSC-measurement starts with the native protein at 35 °C and decreases to -14 °C. Simulations with 3 different models. Magenta lines: $\Theta_U(T)$ -weighted chemical equilibrium two-state model. $\Delta H_0 = -42$ kcal/mol. $\Delta C_p^0 = 1.1$ kcal/molK. Red lines: statistical-mechanical two-state model. $\Delta E_0 = -42$ kcal/mol, $C_v = 0.45$ kcal/molK. Green lines: multistate cooperative model. $h_0 = -360$ cal/mol, $c_v = 4.0$ cal/molK, $\sigma = 8 \times 10^{-5}$, $N = 160$. (A) Heat capacity. (B) Enthalpy/inner energy. (C) Entropy. (D) Free energy.

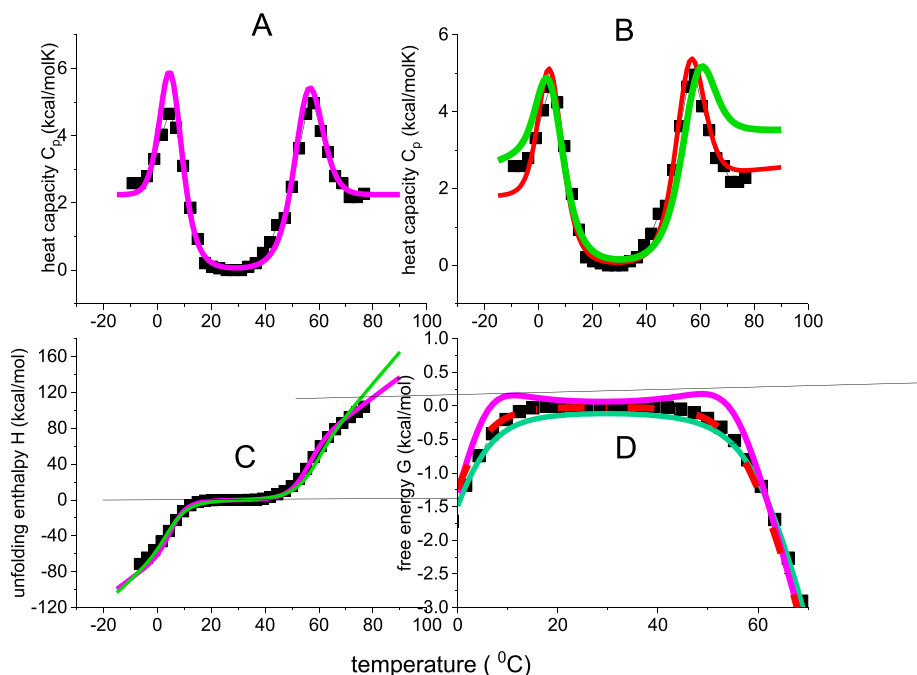


Figure 7. Heat-induced folding (at 4 °C) and unfolding (at 57 °C) of β -lactoglobulin in 2.0 M urea solution. DSC heat capacity data (black squares in panels A and B) are taken from ref 41. Black data points in panels C and D correspond to the red data points in Figure 3B,D. Magenta lines: $\Theta_U(T)$ -weighted chemical equilibrium two-state model. $\Delta H_0 = 56$ kcal/mol; $\Delta C_p^0 = 2.25$ kcal/molK. Red lines: statistical-mechanical two-state model. $\Delta E_0 = 55$ kcal/mol; $C_v = 1.15$ kcal/molK. Green lines: multistate cooperative model. $h_0 = 0.58$ kcal/mol, $c_v = 17$ cal/molK, $\sigma = 7 \times 10^{-5}$, $N = 80$.

considerable differences between the van't Hoff enthalpy of spectroscopy and the calorimetric unfolding enthalpy. The van't Hoff enthalpy ΔH_0 derived with eq 10 was typically 20–50%

smaller than the calorimetric ΔH_{DSC} (see ref 1, Table 2). The analysis of the spectroscopic experiment becomes even more ambiguous if heat and cold denaturation are reported in the

same experiment. This is illustrated for an NMR experiment with frataxin^{43,49} in the [Supporting Information](#). Correct thermodynamic conclusions can only be made by comparison to DSC experiments.

Two-state models are simple approximations to cooperative protein unfolding. A large ensemble of micro-states is replaced by just two macro-states. The native and the unfolded protein conformation are assumed to be separated by a high free energy barrier and intermediate conformations are not populated. Intuitively, a two-state model is considered as the most cooperative limit of protein unfolding. However, it should be realized that the formalism of two-state unfolding contains no element of molecular cooperative interactions. Indeed, the statistical-mechanical two-state model follows from the cooperative multi-state model in the limit of no cooperativity.²⁶

$\Theta_U(T)$ -Weighted Chemical Equilibrium Two-State Model. The standard model (eqs 7–11) correctly simulates the heat capacity $C_p(T)$, but fails for enthalpy, entropy and free energy. This is corrected here by multiplying the thermodynamic functions with the extent of unfolding $\Theta_U(T)$, leading to the $\Theta_U(T)$ -weighted functions 11–14. These thermodynamic relations simulate all experimental data quite well (magenta lines in [Figures 2](#) and [5](#)). In particular, the parabolic free energy of the standard chemical equilibrium model (eq 9) is replaced by a trapezoidal temperature profile (eq 14). However, as shown in [Figures 4–7](#), the agreement between DSC and the $\Theta_U(T)$ -weighted chemical equilibrium model is not perfect. The model predicts small positive free energies in the vicinity of the midpoints of unfolding, which is not supported by the experimental data.

Statistical-Mechanical Two-State Model. The DSC experiment is intimately related to the protein partition function.^{4,9,25,28,50,51} The partition function $Z(T)$ (eq 19) describes all thermodynamic properties. $Z(T)$ follows from the Ising model²⁴ as modified in [ref 4, 25](#). The inner energy ΔE_0 of the statistical-mechanical two-state model is almost identical to the conformational enthalpy ΔH_0 of the chemical equilibrium model. However, no assumption about the entropy is required, which is in contrast to the chemical equilibrium two-state model (eq 8).²⁶ The statistical-mechanical two-state model predicts a trapezoidal temperature profile of the free energy, which is in excellent agreement with the DSC experiments. The free energy is zero or negative, never positive. The molecular multistate partition function (eq 22) reduces to eq 19 if the cooperativity parameter is $\sigma = 1$ (= no cooperativity).²⁶

Multistate Cooperative Model.¹⁶ The model is based on molecular parameters only. The unfolding enthalpy per amino acid residue is typically $h_0 \sim 0.9$ – 1.3 kcal/mol.¹ This is confirmed by lysozyme with $h_0 = 0.9$ kcal/mol. In contrast, β -lactoglobulin has low h_0 -values of 0.38–0.58 kcal/mol, probably caused by the high content of β -structure (cf. [ref 52](#)). Multiplying h_0 with the number of unfolded amino acid residues n yields an approximate conformational enthalpy $\Delta H_0 = 60.8$ kcal/mol.

Protein unfolding is a dynamic equilibrium of many short-lived intermediates, the probability of which is determined by the cooperativity parameter σ . Lysozyme unfolding is highly cooperative with a correspondingly small $\sigma = 5 \times 10^{-7}$. The probability of intermediates is distinctly reduced and lysozyme is the classical example for an apparent two-state unfold. The cooperativity parameter σ is a physically well-defined quantitative measure of cooperativity (see below).

Protein Stability and Free Energy. The basic tenet in protein folding is the assumption that proteins spontaneously fold into their native conformation. In the folding funnel hypothesis, the native proteins sit in a free energy minimum at the bottom of a rough-walled funnel. The folding process is a balanced enthalpy-entropy compensation. It involves a reduction in conformational entropy compensated by a gain in inner energy, resulting in a minimal free energy in favor of the folded structure. The common range of this minimal free energy that is quoted in the literature is 5–15 kcal/mol.⁴⁰ The folding funnel is rather shallow^{53,54} and because of their small free energies of unfolding, proteins are often said to be only “marginally stable.”⁵⁵

However, the free energy may not be the best criterion to judge protein stability. The trapezoidal free energy profile of β -lactoglobulin ([Figures 3D](#) and [7D](#)) resembles an inverted “funnel.” The free energy change of the urea-destabilized protein is -3 kcal/mol at 4 °C and -4.35 kcal/mol at 57 °C. Interestingly, the free energy change of the more stable globular lysozyme is almost identical with -4.27 kcal/mol at 72 °C. The free energy allows no differentiation in the stability of the two proteins.

Alternative parameters may be better suited for defining stability. First, and most important is the midpoint temperature of heat unfolding T_m . DSC measures directly and independent of any folding model, the unfolding enthalpy ΔH_{DSC} and the unfolding entropy ΔS_{DSC} . The ratio of these thermodynamic parameters defines the midpoint temperature T_m assuming a first-order phase transition

$$T_m = \frac{\Delta H_{DSC}}{\Delta S_{DSC}}, \frac{\Delta H_{\Theta_{total}}}{\Delta S_{\Theta_p}}, \frac{\Delta E_{total}}{\Delta S_v} \quad (27)$$

[Table 1](#) shows the excellent agreement between the measured T_m and the predictions according to eq 27. A large unfolding enthalpy and a small entropy shift T_m to high temperatures. [Equation 27](#) is equally applicable to T_{cold} as demonstrated for cold denaturation of β -lactoglobulin (cf. [Table 1](#)). Upon cold denaturation, the unfolding enthalpy of β -lactoglobulin is reduced by 30%, but the entropy by only 10%. The combined effect of these rather small changes is a reduction in unfolding temperature by 54 °C.

A second stability criterion is the temperature difference between heat and cold denaturation.⁵⁵ The DSC experiment reveals a trapezoidal temperature profile of the free energy ([Figures 3D](#) and [5D](#)). The temperature difference between heat and cold denaturation, $\Delta T = T_m - T_{cold}$, can be measured under favorable circumstances, but is usually not available experimentally. However, the $\Theta_U(T)$ -weighted chemical equilibrium model predicts $\Delta T \approx 2T_0(1 - e^{-\Delta H_0/T_0\Delta C_p^0})$, the statistical-mechanical two-state model $\Delta T = \frac{\Delta E_0}{C_v}$, and the multistate cooperative model $\Delta T \approx \frac{h_0}{c_v}$. In all models the temperature difference ΔT increases with the conformational enthalpy ΔH_0 , inner energy ΔE_0 and h_0 , and decreases with increasing heat capacities ΔC_p^0 , C_v , and c_v . A large heat capacity corresponds to large energy fluctuations (eq 18), reducing the protein stability.

A third stability parameter is the width of the heat capacity peak itself. This is ~ 28 °C for lysozyme and 43 °C for urea-destabilized β -lactoglobulin. The width of the transition peak reflects the strength of the intramolecular interactions and, in turn, the cooperativity of the system. A broad peak corresponds

to a low cooperativity and a looser protein structure, whereas a sharp peak indicates a very cooperative system. A quantitative measure is the cooperativity parameter σ . The free energy to start a new folded sequence within an unfolded domain (nucleation) is given by $\Delta G_\sigma = -RT \ln \sigma$. For lysozyme ($\sigma = 5 \times 10^{-7}$) ΔG_σ is 9.6 kcal/mol, for β -lactoglobulin ($\sigma = 7 \times 10^{-5}$) the nucleation energy is 6.2 kcal/mol. These are large barriers for the initiation of new structures. The larger the nucleation energy, the more stable is the protein. The two proteins have almost identical free energies of unfolding, but their nucleation energies differ by 3.2 kcal/mol in favor of the more stable lysozyme.

Similar large free energies of structure initiation have been found in molecular dynamics calculations.^{56,57} The last comparison shows that the model-free analysis of thermodynamic unfolding data is not only important to test simple models but may also be applied to the more advanced molecular dynamics results as, for example, described in the “dynamoeconomics entropy dictionary.”³⁹

CONCLUDING REMARKS

The important thermodynamic properties for protein unfolding are enthalpy, entropy and free energy. These parameters can be obtained by measuring the heat capacity with differential scanning calorimetry, followed by integration of the thermograms. No unfolding model is needed. Rather on the contrary, the experimental temperature profiles $\Delta H(T)_{\text{DSC}}$, $T\Delta S(T)_{\text{DSC}}$, and $\Delta G(T)_{\text{DSC}}$ are necessary to test unfolding models, be it two-state unfolding or multistate cooperative unfolding. DSC experiments of lysozyme and β -lactoglobulin are presented. Enthalpy and entropy display sigmoidal temperature profiles while the free energy has a trapezoidal shape as observed experimentally for β -lactoglobulin. The experimental results are analyzed with two new two-state models, the $\Theta_U(T)$ -weighted chemical equilibrium model and the statistical-mechanical model, and a multistate cooperative model. The standard chemical equilibrium model with its parabolic free energy profile does not fit the experimental data. Two-state models are suited for small proteins and provide macroscopic thermodynamic parameters. Molecular insight is gained only by applying a multistate cooperative model.

ASSOCIATED CONTENT

Supporting Information

The Supporting Information is available free of charge at <https://pubs.acs.org/doi/10.1021/acs.jpccb.3c00882>.

The supporting information compares the interpretation of the spectroscopic protein unfolding experiment with two different two-state models (PDF)

AUTHOR INFORMATION

Corresponding Author

Joachim Seelig – Biozentrum, University of Basel, CH-4056 Basel, Switzerland; orcid.org/0000-0001-8564-104X; Phone: +41-61 207 2190; Email: joachim.seelig@unibas.ch

Author

Anna Seelig – Biozentrum, University of Basel, CH-4056 Basel, Switzerland; orcid.org/0000-0003-3509-2569

Complete contact information is available at: <https://pubs.acs.org/10.1021/acs.jpccb.3c00882>

Funding

Stiftung zur Förderung der biologischen Forschung, Basel, Switzerland.

Notes

The authors declare no competing financial interest.

REFERENCES

- (1) Seelig, J.; Schönfeld, H.-J. Thermal protein unfolding by differential scanning calorimetry and circular dichroism spectroscopy. Two-state model versus sequential unfolding. *Quart. Rev. Biophys.* **2016**, *49*, No. e9.
- (2) Jackson, W. M.; Brandts, J. F. Thermodynamics of protein denaturation - a calorimetric study of reversible denaturation of chymotrypsinogen and conclusions regarding accuracy of 2-state approximation. *Biochemistry* **1970**, *9*, 2294–2301.
- (3) Privalov, P. L.; Khechinashvili, N. N. Thermodynamic approach to problem of stabilization of globular protein structure - calorimetric study. *J. Mol. Biol.* **1974**, *86*, 665–684.
- (4) Zimm, B. H.; Bragg, J. K. Theory of the phase transition between helix and random coil in polypeptide chains. *J. Chem. Phys.* **1959**, *31*, 526–535.
- (5) Brandts, J. F. Thermodynamics of protein denaturation. I. Denaturation of chymotrypsinogen. *J. Am. Chem. Soc.* **1964**, *86*, 4291–4301.
- (6) Privalov, P. L. Cold denaturation of proteins. *Crit. Rev. Biochem. Mol. Biol.* **1990**, *25*, 281–306.
- (7) Privalov, P. L. Thermodynamics of protein folding. *J. Chem. Thermodyn.* **1997**, *29*, 447–474.
- (8) Ibarra-Molero, B.; Naganathan, A.; Sanchez-Ruiz, J. M.; Munoz, V. Modern analysis of protein folding by differential scanning calorimetry. In *Methods in enzymology*; Elsevier, 2016; pp 281–316.
- (9) Zhou, Y.; Hall, C. K.; Karplus, M. The calorimetric criterion for a two-state process revisited. *Protein Sci.* **1999**, *8*, 1064–1074.
- (10) Chen, C. R.; Makhatazde, G. I. Molecular determinant of the effects of hydrostatic pressure on protein folding stability. *Nat. Commun.* **2017**, *8*, 14561.
- (11) Makhatazde, G. I.; Privalov, P. L. Energetics of protein structure. *Adv. Protein Chem.* **1995**, *47*, 307–425.
- (12) Becktel, W. J.; Schellman, J. A. Protein stability curves. *Biopolymers* **1987**, *26*, 1859–1877.
- (13) Schellman, J. A. The thermodynamic stability of proteins. *Annu. Rev. Biophys. Chem.* **1987**, *16*, 115–137.
- (14) Gomez, J.; Hilsner, V. J.; Xie, D.; Freire, E. The heat-capacity of proteins. *Proteins: Struct., Funct., Genet.* **1995**, *22*, 404–412.
- (15) Myers, J. K.; Pace, C. N.; Scholtz, J. M. Denaturant m values and heat capacity changes: relation to changes in accessible surface areas of protein unfolding. *Protein Sci.* **1995**, *4*, 2138–2148.
- (16) Seelig, J.; Seelig, A. Molecular understanding of calorimetric protein unfolding experiments. *Biophys. Rep.* **2022**, *2*, No. 100037.
- (17) Durowoju, I. B.; Bhandal, K. S.; Hu, J.; Carpick, B.; Kirkitadze, M. Differential scanning calorimetry - A method for assessing the thermal stability and conformation of protein antigen. *J. Vis. Exp.* **2017**, *121*, 55262.
- (18) Privalov, P. L.; Dragan, A. I. Microcalorimetry of biological macromolecules. *Biophys. Chem.* **2007**, *126*, 16–24.
- (19) Onuchic, J. N.; LutheySchulten, Z.; Wolynes, P. G. Theory of protein folding: The energy landscape perspective. *Annu. Rev. Phys. Chem.* **1997**, *48*, 545–600.
- (20) Portman, J. J.; Takada, S.; Wolynes, P. G. Microscopic theory of protein folding rates. I. Fine structure of the free energy profile and folding routes from a variational approach. *J. Chem. Phys.* **2001**, *114*, 5069–5081.
- (21) Baumann, R. P. Evaluation of thermodynamic properties. In *Modern Thermodynamics with Statistical Mechanics*; McConnin, R. A., Ed.; Macmillan Publishing Company: New York, USA, 1992; p 341.
- (22) Eisenberg, D.; Crothers, D. Calculation of the energy using the sysem partition function. In *Physical Chemistry with Applications to the*

Life Sciences; Rhame, B., Moore, M., Eds.; The Benjamin/Cummings Publishing Company, Inc.: Menlo Park, CA, 1979; p 675.

(23) Sirotkin, V. A.; Winter, R. Volume changes associated with guanidine hydrochloride, temperature, and ethanol induced unfolding of lysozyme. *J. Phys. Chem. B* **2010**, *114*, 16881–16886.

(24) Ising, E. Report on the theory of ferromagnetism. *Z. Phys.* **1925**, *31*, 253–258.

(25) Davidson, N. *Statistical Mechanics*; Mac Graw-Hill: New York, 1962; p 385.

(26) Li-Blatter, X.; Seelig, J. Thermal and chemical unfolding of lysozyme. Multistate Zimm-Bragg theory versus two-state model. *J. Phys. Chem. B* **2019**, *123*, 10181–10191.

(27) Zimm, B. H.; Doty, P.; Iso, K. Determination of the parameters for helix formation in poly-gamma-benzyl-L-glutamate. *Proc. Natl. Acad. Sci. U. S. A.* **1959**, *45*, 1601–1607.

(28) Zimm, B. H.; Rice, S. A. The helix-coil transition in charged macromolecules. *Mol. Phys.* **1960**, *3*, 391–407.

(29) Zehender, F.; Ziegler, A.; Schonfeld, H. J.; Seelig, J. Thermodynamics of protein self-association and unfolding. The case of apolipoprotein A-I. *Biochemistry* **2012**, *51*, 1269–1280.

(30) Schulthess, T.; Schonfeld, H. J.; Seelig, J. Thermal unfolding of apolipoprotein A-1. Evaluation of methods and models. *Biochemistry* **2015**, *54*, 3063–3075.

(31) Seelig, J. Cooperative protein unfolding. A statistical-mechanical model for the action of denaturants. *Biophys. Chem.* **2018**, *233*, 19–25.

(32) Eckhardt, D.; Li-Blatter, X.; Schonfeld, H. J.; Heerklotz, H.; Seelig, J. Cooperative unfolding of apolipoprotein A-1 induced by chemical denaturation. *Biophys. Chem.* **2018**, *240*, 42–49.

(33) Garidel, P.; Eiperle, A.; Blech, M.; Seelig, J. Thermal and chemical unfolding of a monoclonal IgG1 antibody: application of the multistate Zimm-Bragg theory. *Biophys. J.* **2020**, *118*, 1067–1075.

(34) Seelig, J. Free energy in thermal and chemical protein unfolding. In *Gibbs energy and Helmholtz energy: Liquids, Solutions and Vapours*; Wilhelm, E., Letcher, T. M., Eds.; Royal Society of Chemistry: London, 2022; pp 363–378.

(35) Privalov, P. L.; Gill, S. J. Stability of protein-structure and hydrophobic interaction. *Adv. Protein Chem.* **1988**, *39*, 191–234.

(36) Privalov, P. L.; Makhatadze, G. I. Heat capacity of proteins. II. Partial molar heat capacity of the unfolded polypeptide chain of proteins: protein unfolding effects. *J. Mol. Biol.* **1990**, *213*, 385–391.

(37) Privalov, G.; Kavina, V.; Freire, E.; Privalov, P. L. Precise scanning calorimeter for studying thermal-properties of biological macromolecules in dilute-solution. *Anal. Biochem.* **1995**, *232*, 79–85.

(38) Rosgen, J.; Hinz, H. J. Response functions of proteins. *Biophys. Chem.* **2000**, *83*, 61–71.

(39) Towse, C. L.; Akke, M.; Daggett, V. The dynamomics entropy dictionary: a large-scale assessment of conformational entropy across protein fold space. *J. Phys. Chem. B* **2017**, *121*, 3933–3945.

(40) Sorokina, I.; Mushegian, A. R.; Koonin, E. V. Is protein folding a thermodynamically unfavorable, active, energy-dependent process? *Int. J. Mol. Sci.* **2022**, *23*, 521.

(41) Griko, Y. V.; Privalov, P. L. Calorimetric study of the heat and cold denaturation of beta-lactoglobulin. *Biochemistry* **1992**, *31*, 8810–8815.

(42) Dreydoppel, M.; Balbach, J.; Weininger, U. Monitoring protein unfolding transitions by NMR-spectroscopy. *J. Biomol. NMR* **2022**, *76*, 3–15.

(43) Pastore, A.; Martin, S. R.; Politou, A.; Kondapalli, K. C.; Stemmler, T.; Temussi, P. A. Unbiased cold denaturation: Low- and high-temperature unfolding of yeast frataxin under physiological conditions. *J. Am. Chem. Soc.* **2007**, *129*, 5374–5375.

(44) Nicholson, E. M.; Scholtz, J. M. Conformational stability of the *Escherichia coli* HPr protein: test of the linear extrapolation method and a thermodynamic characterization of cold denaturation. *Biochemistry* **1996**, *35*, 11369–11378.

(45) Svilenov, H. L.; Menzen, T.; Richter, K.; Winter, G. Modulated scanning fluorimetry can quickly assess thermal protein unfolding reversibility in microvolume samples. *Mol. Pharmaceutics* **2020**, *17*, 2638–2647.

(46) Hedoux, A.; Krenzlín, S.; Paccou, L.; Guinet, Y.; Flament, M. P.; Siepmann, J. Influence of urea and guanidine hydrochloride on lysozyme stability and thermal denaturation; a correlation between activity, protein dynamics and conformational changes. *PCCP* **2010**, *12*, 13189–13196.

(47) Stadler, A. M.; Demmel, F.; Ollivier, J.; Seydel, T. Picosecond to nanosecond dynamics provide a source of conformational entropy for protein folding. *Phys. Chem. Chem. Phys.* **2016**, *18*, 21527–21538.

(48) Stadler, A. M.; Koza, M. M.; Fitter, J. Determination of conformational entropy of fully and partially folded conformations of holo- and apomyoglobin. *J. Phys. Chem. B* **2015**, *119*, 72–82.

(49) Sanfelice, D.; Morandi, E.; Pastore, A.; Niccolai, N.; Temussi, P. A. Cold denaturation unveiled: molecular mechanism of the asymmetric unfolding of yeast frataxin. *Chem. Phys. Chem.* **2015**, *16*, 3599–3602.

(50) Freire, E.; Biltonen, R. L. Statistical mechanical deconvolution of thermal transitions in macromolecules. 1. Theory and application to homogeneous systems. *Biopolymers* **1978**, *17*, 463–479.

(51) Munoz, V.; Sanchez-Ruiz, J. M. Exploring protein-folding ensembles: A variable-barrier model for the analysis of equilibrium unfolding experiments. *Proc. Natl. Acad. Sci. U. S. A.* **2004**, *101*, 17646–17651.

(52) Meier, M.; Seelig, J. Thermodynamics of the coil \rightleftharpoons beta-sheet transition in a membrane environment. *J. Mol. Biol.* **2007**, *369*, 277–289.

(53) Taverna, D. M.; Goldstein, R. A. Why are proteins marginally stable? *Proteins: Struct., Funct., Genet.* **2002**, *46*, 105–109.

(54) Wilson, A. E.; Kosater, W. M.; Liberles, D. A. Evolutionary processes and biophysical mechanisms: revisiting why evolved proteins are marginally stable. *J. Mol. Evol.* **2020**, *88*, 415–417.

(55) Sanfelice, D.; Temussi, P. A. Cold denaturation as a tool to measure protein stability. *Biophys. Chem.* **2016**, *208*, 4–8.

(56) Yang, A. S.; Honig, B. Free energy determinants of secondary structure formation: I. alpha-Helices. *J. Mol. Biol.* **1995**, *252*, 351–365.

(57) Yang, A. S.; Honig, B. Free-energy determinants of secondary structure formation. 2. Antiparallel beta-sheets. *J. Mol. Biol.* **1995**, *252*, 366–376.